

Short Communication

## Rapid Determination of Rhodamine B in Chilli Powder by Electrochemical Sensor Based on Graphene Oxide Quantum Dots

Weiguo Liu<sup>1</sup>, Xin Wei<sup>1</sup>, Zhaoxia Wang<sup>2</sup>, Ganghui Chu<sup>1,\*</sup>, Xueliang Wang<sup>2,\*\*</sup>

<sup>1</sup> College of Chemistry and Environmental Science, Kashi University, 844000, PR China.

<sup>2</sup> School of Chemistry and Chemical Engineering, Heze University, 274015, PR China.

\*E-mail: [cghks5@126.com](mailto:cghks5@126.com)

\*\*E-mail: [qust-1977wxl@163.com](mailto:qust-1977wxl@163.com)

Received: 16 September 2022 / Accepted: 6 November 2022 / Published: 17 November 2022

---

A novel method for determination of rhodamine B (Rh B) was proposed based on a glassy carbon electrode modified graphene oxide quantum dots (GOQDs/GCE). Compared with that on the bare GCE, the oxidation peak current of Rh B increased significantly and the oxidation over potential decreased on the GOQDs/GCE, indicating that the GOQDs have a good catalytic effect on the electrochemical oxidation of Rh B. Under the optimal conditions, the oxidation current of Rh B showed a good linear relationship with its concentration in the range of 5.0 ~ 50.0  $\mu\text{M}$  with the correlation coefficient (R) of 0.9955, and the detection limit of 0.80  $\mu\text{M}$  was obtained (S/N = 3). The proposed sensor can be used for detection of Rh B in chilli powder with the advantages of good stability and satisfactory percent recovery.

---

**Keywords:** Graphene oxide quantum dots; Electrochemical sensor; Rhodamine B; Differential pulse voltammetry

### 1. INTRODUCTION

As an important kind of food additive, food colorants are widely used for food color bright [1]. The food colorants are generally divided into natural colorants and synthetic colorants. These two kinds of food colorants have their individual advantages. The natural colorants that are from natural products have less toxicity and less harmfulness compare with the synthetic colorants, however, the natural colorants are less stable and the price is more expensive. The synthetic colorants are more widely used not only because they are cheap, but they have many tones, bright stable color, strong coloring power, and they are easy to be used [2].

Rhodamine B (Rh B), as a synthetic colorant, is a triphenylmethane basic water-soluble dye (The chemical structure is shown in the Figure 1.). Because of its stable coloring and low production cost, some illegal traders add Rh B to food to increase its color. However, Rh B can lead to acute or chronic poisoning symptoms such as headache, nausea and limb weakness occur in the body [3, 4]. Rh B is a kind of carcinogen, genotoxic substance and animal neurotoxic substance [5], and it has been listed as the third carcinogen by the International Agency for Research on Cancer in 1987, and listed as illegal food additive by EU and China [6,7]. Therefore, the establishment of a rapid and efficient detection method for Rh B is of great significance to food safety and human health.

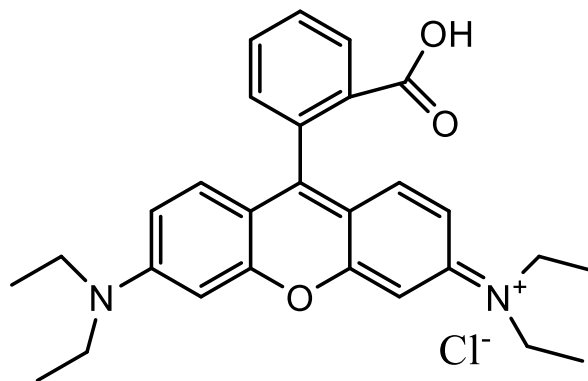


**Figure 1.** Chemical structure of Rhodamine B

At present, the most commonly used analytical methods for Rh B are liquid chromatography [8-11], spectrophotometry [12-14], liquid chromatography-mass spectrometry [15-17], UV-vis spectroscopy [18] and fluorescence spectrometry [19]. However, most of these methods require expensive instruments, complex operation, and the detection process contains a large number of toxic organic solvents. In contrast, electrochemical methods are widely used in food safety analysis because of their low cost, simple operation, rapid analysis, high accuracy and sensitivity [20-23]. Based on Rh B has good electrochemical activity, so it can be detected directly by electrochemical methods. Unfortunately, as far as we know, the literature on electrochemical determination of Rh B is relative scanty. For example, Yu et al. [24] reported a simple voltammetric assay for rhodamine B using a bare glassy carbon electrode (GCE). The anodic peak current of rhodamine B is linear with its concentration in the range of 4.78 ~ 956.1  $\mu\text{g L}^{-1}$ , and the detection limit was 2.93  $\mu\text{g L}^{-1}$ . However, this method was confined from its low sensitivity and selectivity. To improve the electrochemical sensing performance, chemically modified electrode was nowadays usually used strategy in electrochemical sensors and variety of nanomaterials have been developed [25-27]. Zhang et al. [28] established a sensitive and simple electrochemical method for the determination of rhodamine B on a silica-pillared zirconium phosphate/nafion composite (SPZP/NAF) composite modified electrode. Because of the layered structure and large specific surface area of SPZP, the SPZP/NAF modified electrode showed high electrocatalytic activity for the oxidation of rhodamine B. Under the optimum conditions, the linear response range of SPZP/NAF modified electrode to rhodamine B is 0.01 ~ 5.0  $\mu\text{M}$ , and the detection limit was 4.3 nM. Sun et al. [29] established a sensitive, rapid and simple electrochemical sensor for the determination of Rh B based on the sensitizing effect of N-methyl-2-pyrrolidone (NMP) on exfoliated

graphene nanowires (GS). On the surface of NMP stripped GS modified electrode, the oxidation signal of Rh B was greatly enhanced, thus the detection sensitivity was significantly improved. The linear range of this method is 5.0~120.0 nM and the detection limit was 1.5 nM. Yi et al. [30] prepared per-6-thio- $\beta$ -cyclodextrin functionalized nanogold/hollow carbon nanospheres ( $\beta$ -Cd-AuNPs/HCNS) nano-hybrid materials and these materials are used to determination of Rh B in the concentration of 4.79-958.00  $\mu\text{g L}^{-1}$  with the detection limit of 0.96  $\mu\text{g L}^{-1}$ . because HCNS has excellent electrochemical properties and large specific surface area, and  $\beta$ -CD has high host-guest recognition and highwater solubility, as well as AuNPs has good electrocatalytic activity.

Graphene is a kind of new carbon nanomaterial, which has been widely used in the construction of electrochemical sensors because of its large specific surface area, good chemical stability, unique electronic and mechanical properties [31]. Graphene oxide quantum dots (GOQDs), as an important derivative of graphene, contain a large number of oxygen-containing functional groups, which provide rich reaction sites for the application of GOQDs [32], and they have excellent optical and electrical properties, such as photoluminescence, high specific surface area and electrical conductivity [33-36] due to the special boundary effect and quantum confinement effect. Therefore, the electrochemical sensors based on the graphene quantum dots [37] have been widely studied and applied. However, there are no reports about the use of graphene oxide quantum dots in Rh B detection.

In this research, graphene oxide quantum dots (GOQDs) were coated on the surface of glassy carbon electrode (GCE) to construct GOQDs/GCE electrochemical sensor. GOQDs was characterized by scanning electron microscope (SEM) and infrared spectroscopy (IR). GOQDs/GCE electrode has good electrochemical catalytic performance of Rh B, and the concentration of Rh B is proportional to the peak current. The relationship between peak current and Rh B concentration was recorded by differential pulse voltammetry, and the effects of pH value and scanning rate on the performance of the electrode were studied. The prepared GOQDs/GCE electrode has a good application prospect in the detection of Rh B.

## 2. MATERIALS AND METHODS

### 2.1 Instruments and reagents

CHI660E electrochemical workstation (Shanghai Chenhua instrument Co., Ltd.), three-electrode system: silver-silver chloride electrode reference electrode, platinum wire electrode opposite electrode, glassy carbon electrode working electrode; GeminiSEM 300 thermal field emission scanning electron microscope (SEM) (Karl Zeiss Optics Co., Ltd., Germany); Nicolet iS50 Fourier transform infrared spectrometer (Seamer Fischer Technology Molecular Spectroscopy, USA). KH-100DB numerical control ultrasonic cleaner (Kunshan Hechuang Ultrasonic instrument Co., Ltd., China); PHSJ- 5 pH meter (Shanghai instrument Electric Scientific instrument Co., Ltd., China).

Graphene oxide quantum dots (Nanjing Xianfeng Nanomaterial Technology Co., Ltd., China); Rhodamine B (Shanghai McLean biochemical Technology Co., Ltd., China). All the reagents used were analytically pure and the water used in the experiment was ultra-pure water.

## 2.2 Preparation of modified electrode

### 2.2.1 Pretreatment of glassy carbon electrode

The bare glassy carbon electrode (diameter 3 mm) was polished into a mirror with 0.05  $\mu\text{m}$   $\text{Al}_2\text{O}_3$  suspension on suede leather, then washed with anhydrous ethanol and distilled water in turn, and treated with ultrasound at the same time. The above operation was repeated twice, then washed with secondary distilled water, dried, and set aside.

### 2.2.2 Preparation of graphene oxide Quantum Dots modified electrode

The graphene oxide quantum dot modified GOQDs/GCE electrode was obtained by removing 6.0  $\mu\text{L}$  graphene oxide quantum dots and adding droplets on the surface of the pretreated glassy carbon electrode and drying under infrared lamp.

### 2.2.3 Electrochemical detection

First of all, the electrode was put into the electrolytic cell containing 10 mL 0.1 M KCl and 5.0 mM  $\text{K}_3[\text{Fe}(\text{CN})_6]$  solution to ensure that the three-electrode system was installed well. The performance of the modified electrode was characterized by cyclic voltammetry (CV) (- 0.1 ~ 0.6 V) and AC impedance technique. The solution containing different concentrations of rhodamine B was placed in the electrolytic cell by differential pulse voltammetry and the electrochemical detection was carried out at 25  $^\circ\text{C}$ .

## 3. RESULTS AND DISCUSSION

### 3.1 Characterization of graphene oxide Quantum Dots

The SEM image of the electrode surface was observed by GeminiSEM300 thermal field emission scanning electron microscope. Figure 2 (A) shows the surface image of GOQDs/GCE. When the GOQDs was modified on the clean GCE, the surface of the GCE was covered with a layer of uniform film, which are consistent with the literature of [38]. The carboxyl and hydroxyl groups of GOQDs are rich in negative charge in aqueous solution, which prevents them from accumulating. The results showed that GOQDs was successfully modified on the surface of GCE.

Figure 2 (B) shows the infrared spectrum of graphene oxide quantum dots. It can be seen from the figure that GOQDs has a broad and strong absorption peak near 3300  $\text{cm}^{-1}$ , which belongs to the stretching vibration peak of O-H, and the absorption peak at 1640  $\text{cm}^{-1}$  may belong to the bending vibration absorption peak of C-OH and the stretching vibration peak of C=O, indicating that there are abundant -OH and -COOH functional groups in GOQDs under experimental conditions [39, 40].

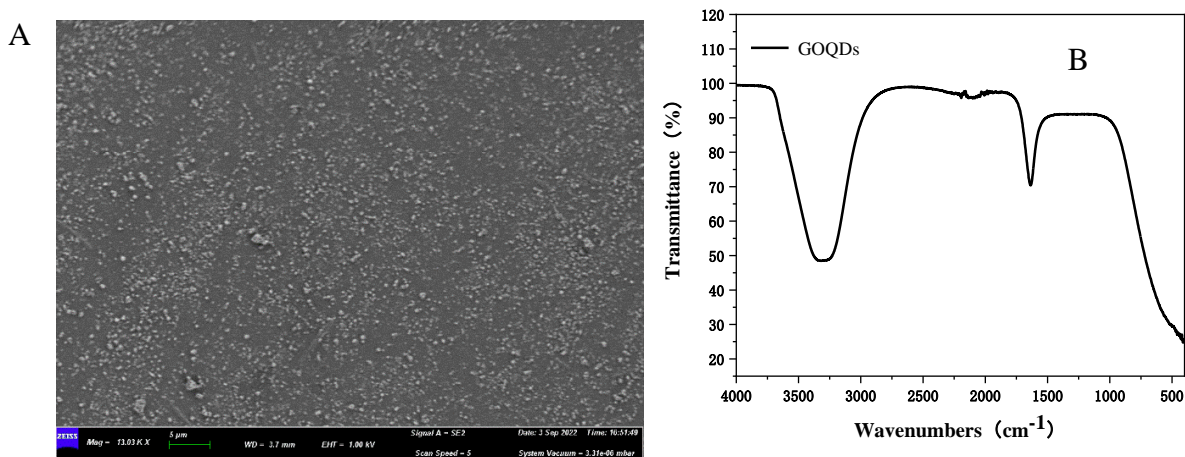


**Figure 2.** Scanning electron microscope (A) and infrared spectrum (B) of graphene oxide quantum dots.

### 3.2 Electrochemical characterization

Figure 3 (A) shows the CV curve of the modified electrode and the bare electrode in 5.0 mM  $K_3[Fe(CN)_6]$  solution, and the scanning rate is set to  $100\text{ mV}\cdot\text{s}^{-1}$ . It can be seen that there are a pair of obvious redox peaks on the naked GCE, while the current decreases on the GOQDs/GCE, which is ascribed to the repulsion of a large number of oxygen-containing functional groups on the surface of GOQDs with  $[Fe(CN)_6]^{3-}$  [41].

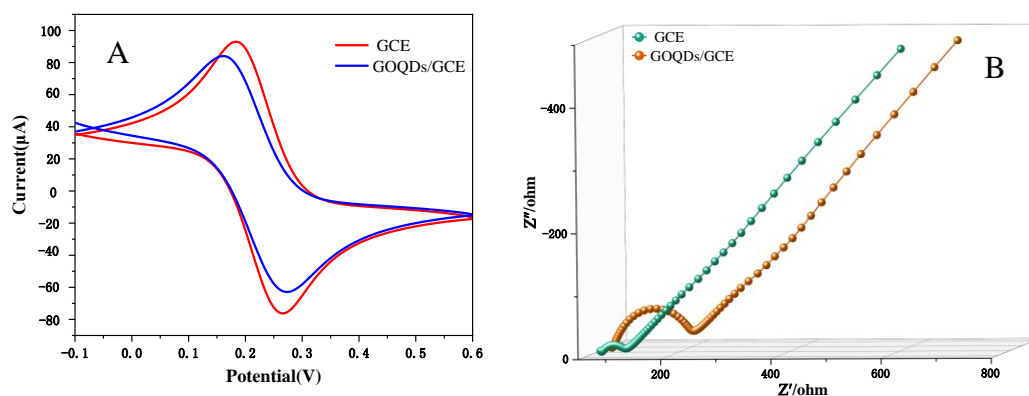


**Figure 3.** (A) CVs and (B) EIS of bare GCE and GOQDs/GCE in a solution which contains 5 mM  $K_3[Fe(CN)_6]$ , 0.1 M KCl (Scan rate is  $100\text{ mV}\cdot\text{s}^{-1}$ ).

The surface changes of the prepared electrodes can be effectively recorded by electrochemical impedance spectroscopy (EIS). Figure 3 (B) shows the AC impedance curves of different electrodes, in which the charge transfer resistance ( $R_{ct}$ ) of GOQDs/GCE is higher than that of bare GCE, which further proves that the resistance increases due to the mutual exclusion between the oxygen-containing functional groups on the surface of GOQDs and  $[Fe(CN)_6]^{3-}$ . Therefore, we can conclude that GOQDs successfully modified the surface of GCE.

### 3.3 Study on Electrochemical behavior of Rh B on GOQDs/GCE electrode

In a buffer solution containing 20  $\mu\text{M}$  rhodamine B, the electrochemical response of Rh B at different electrodes was studied by cyclic voltammetry (Figure 4.). No obvious Rh B oxidation peak (curve a) was observed on the GCE electrode, indicating that naked GCE had no effect on the oxidation of Rh B. On GOQDs/GCE, an irreversible oxidation peak (curve b) is shown at 0.96 V. The experimental results show that GOQDs has good electrocatalytic effect on Rh B.

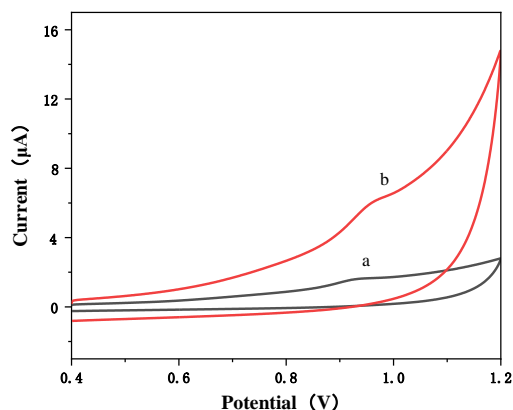


**Figure 4.** CV curves of GCE (a) and GOQDs (b) in 0.2 M PBS (pH= 6.0) containing 20  $\mu\text{M}$  Rh B at a scan rate of  $100 \text{ mV}\cdot\text{s}^{-1}$ .

### 3.4 Effect of pH

We carried out a series of experiments to enhance the electrocatalytic activity of PBS by optimizing the pH value of Rh B buffer solution. Figure 5 (A) shows that the oxidation peak current increases with the increase of pH value (5.5~6.0), and then decreases with the increase of pH value (6.0~7.5). Therefore, the best pH of rhodamine B solution is 6. Figure 5 (B) examines the relationship between the peak potential of rhodamine B and pH. It can be seen from the figure that the peak potential of rhodamine B moves to a negative direction with the increase of pH, and the linear equation of peak potential is  $E_{\text{pa}} (\text{V}) = -0.035 \text{ pH} + 1.112$  ( $r = 0.9969$ ). The slope of the  $dE_{\text{pa}}/d\text{pH}$  curve  $0.035 \text{ pH}^{-1}$  is close to the half of  $0.059 \text{ pH}^{-1}$ , which is equivalent to the stoichiometric ratio of  $1\text{H}^+/2$  electrons [24, 42]. The results show that the electrochemical oxidation of rhodamine B on the electrode is accompanied by proton reaction in the process of electron transfer.

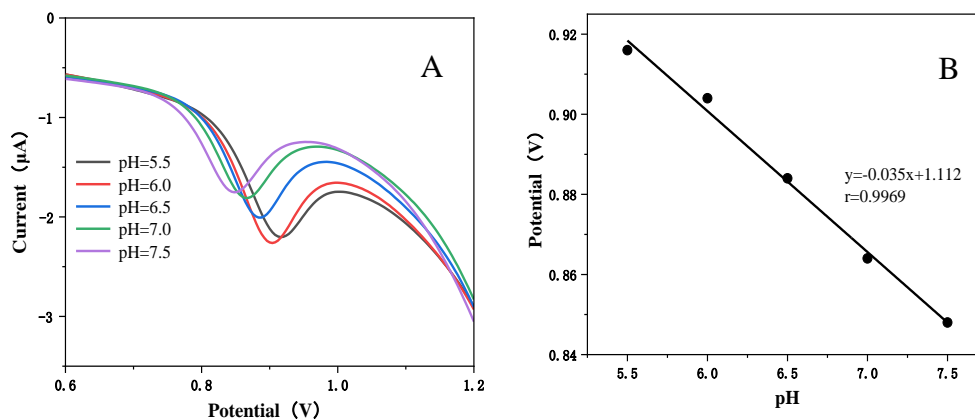


**Figure 5.** In PBS solution containing 20 μM Rh B, the coefficient of variation was obtained by DPV at different pH values of GOQDs/GCE (5.5, 6.0, 6.5, 7.0, 7.5) (A) and the relationship between oxidation peak potential of Rh B and pH value(B).

### 3.5 Effect of scan rates

The effect of different scanning rates on the oxidation peak current of Rh B was investigated by cyclic voltammetry on GOQDs/GCE. The GOQDs/GCE electrode was scanned by cyclic voltammetry in PBS buffer solution containing Rh B at the scanning rates of 20, 30, 40, 50, 60, 70, 80, 90 and 100  $\text{mV}\cdot\text{s}^{-1}$ , respectively. The results are shown in Figure 6. It can be found from the diagram that the peak current increases with the increase of scanning rate, and there is a good linear relationship between the oxidation peak current  $i_{pa}$  (μA) and the scanning rate  $\nu$  ( $\text{mV}\cdot\text{s}^{-1}$ ). The linear fitting equation  $i_{pa} = 0.043\nu + 0.608$  ( $r = 0.9959$ ) shows that the oxidation process of rhodamine B on the electrode surface is controlled by kinetic adsorption process [43]. There is a linear relationship between peak potential (V) and  $\ln \nu$ , and the linear equation is  $E_{pa} = 0.0233 \ln \nu + 0.8570$  ( $r = 0.9880$ ). According to Laviron theory [44], the relationship between  $E_{pa}$  and  $\ln \nu$  can be expressed as follows:

$$E_{pa} = E^0 - \frac{RT}{\alpha nF} \ln \frac{RTK_s}{\alpha nF} + \frac{RT}{\alpha nF} \ln \nu$$

Where  $n$  is the electron transfer number,  $\alpha$  is the electron transfer coefficient,  $K_s$  is the standard rate constant,  $\nu$  is the scanning speed,  $R$  is the gas constant,  $T$  is the temperature, and  $F$  is the Faraday constant. For the irreversible electrode process,  $\alpha$  is assumed to be 0.5, and the number of electrons transferred in the Rh B electrode reaction is calculated to be 2.

Therefore, the oxidation process of Rh B is an irreversible oxidation reaction of two electrons and one proton, which is consistent with the previous literature report [24]. Scheme 1 shows the possible oxidation mechanism of Rh B.

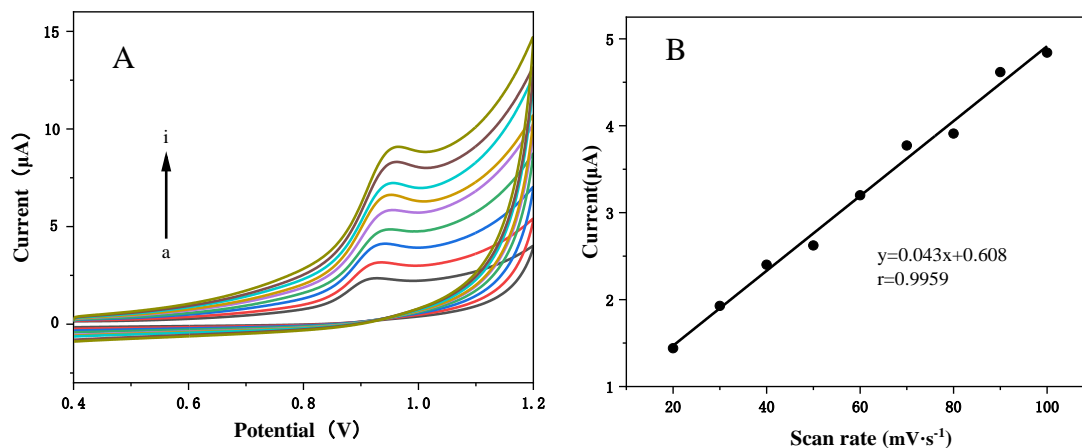
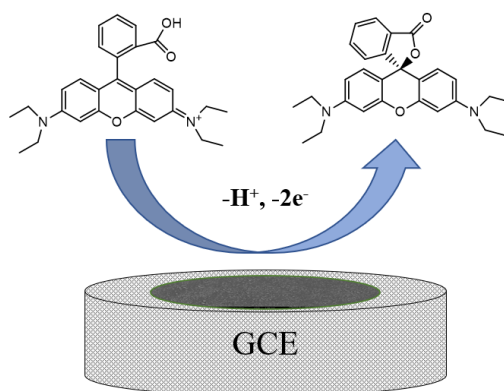


**Figure 6.** The superposed cyclic voltammograms of Rh B at GOQDs/GCE with different scan rates (from a to i, 20、30、40、50、60、70、80、90、100  $\text{mV}\cdot\text{s}^{-1}$ ) (A) and Relationship between scanning rate and oxidation peak current (B).



**Scheme 1.** The oxidation mechanism of Rh B at the GOQDs/GCE.

### 3.6 Linear range and detection limit

Under the best experimental conditions, the relationship between the concentration of Rh B and its peak current was investigated by differential pulse voltammetry. In the concentration range of 5.0~50.0  $\mu\text{M}$ , the peak current of Rh B shows a good linear relationship with the concentration (Figure 7.), and the linear equation is:  $i (\mu\text{A}) = -0.0392C (\mu\text{M}) + 0.0481$ , the correlation coefficient is 0.9955, and the detection limit ( $S/N = 3$ ) is 0.80  $\mu\text{M}$ .

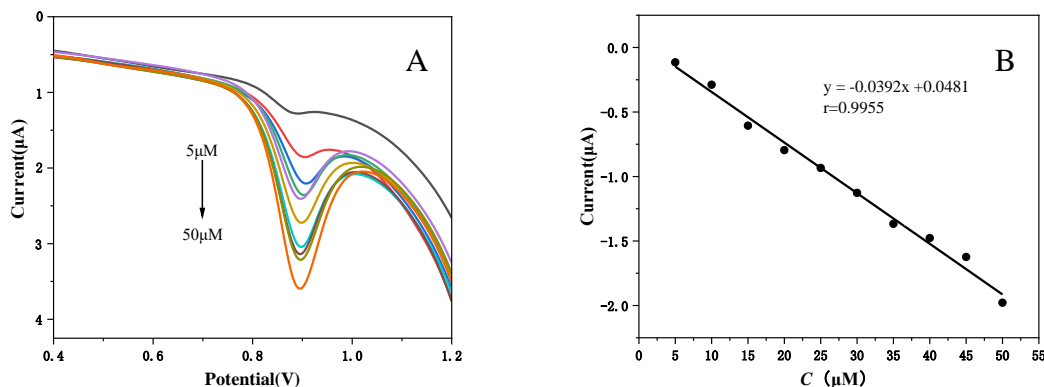


**Figure 7.** DPV of Rh B at modified electrodes. (A) and the plot of peak current versus concentration (B).

In addition, Table 1 lists the comparison between this work and the electrochemical detection methods of Rh B reported in the literature. Although the detection limit is not the lowest, the sensor has obvious advantages in linear range, detection speed and operation, while simplifying the electrode and saving cost.

**Table 1.** Comparison of different chemically modified electrodes for the detection of Rh B

Electrode	Technique	Linea range / ( $\mu\text{M}$ )	Detection limit / ( $\mu\text{M}$ )	Ref.
CQDs/SDBS-OPPy/GCE	SWV	0.05 ~ 10	0.013	[45]
ERGO/ABPE	LSV	0.02 ~ 1.0; 1.0 ~ 8.0	0.01	[46]
Cu@CS/GCE	DPV	0.3 ~ 30.0	0.10	[47]
GOQDs/GCE	DPV	5.0 ~ 50.0	0.80	This work

### 3.7 Reproducibility, Stability and interference experiment of modified electrode

Under the best experimental conditions, the reproducibility of the modified electrode (GOQDs/GCE) was investigated. The relative standard deviation (RSD) of the peak current of Rh B was 3.7% when the concentration of Rh B was determined for 5 times. The results show that the modified electrode has good reproducibility. Five identical modified electrodes were prepared by the same method for experimental determination. The results showed that the electrode had good reproducibility. When the electrode was placed at room temperature for 10 days, the peak potential and peak current were still stable under the same conditions, which indicated that the stability of GOQDs/GCE was good. By premixing Rh B with interfering substances, the effects of coexisting substances such as metal ions, amino acids, carbohydrates and surfactants on the determination method were investigated. Table 2 shows that within the allowable relative error of  $\pm 5\%$ , the presence of  $\text{Zn}^{2+}$ ,  $\text{Mg}^{2+}$ ,  $\text{K}^+$ ,  $\text{Na}^+$ ,  $\text{NO}_3^-$ ,  $\text{SO}_4^{2-}$  and  $\text{Cl}^-$ , sodium citrate, ascorbic acid, glucose, sucrose, glutamic acid and aspartic acid almost

does not interfere with the determination of Rh B.

**Table 2.** Effect of coexisting substances on the determination of 10  $\mu\text{M}$  Rh B

Coexisting substance	Concentration ( $\mu\text{M}$ )	Relative error (%)
$\text{Zn}^{2+}$	500	-3.86
$\text{Mg}^{2+}$	500	-4.30
$\text{K}^+$	500	+1.35
$\text{Na}^+$	500	+1.22
$\text{NO}_3^-$	500	+2.13
$\text{SO}_4^{2-}$	500	-3.47
$\text{Cl}^-$	500	+0.85
sodium citrate	300	-0.69
ascorbic acid	300	+1.22
glucose	300	+1.78
sucrose	300	+3.16
glutamic acid	300	+2.33
aspartic acid	300	+2.08

### 3.8 Actual sample analysis

GOQDs/GCE was applied to the determination of rhodamine B in chili powder. Chili powder was purchased from the local supermarket, 1.0 g sample was taken into the beaker, distilled water of 10 mL was added, 20 min was treated by ultrasonic, and the filtrate was collected in 100 mL volumetric flask. An appropriate amount of sample solution was taken in the electrolytic cell and the pH = 6.0 with PBS, and the content of Rh B in the sample was determined according to the experimental method described in 3.6. The content of Rh B in the sample was determined by the experimental method described in this paper. It was found that there was no oxidation peak of rhodamine B in the sample solution, indicating that the content of Rh B or Rh B in the chili powder samples was lower than the detection limit of this method. The recovery rate was determined by the standard addition method, and the results were shown in Table 3. The calculated recovery rate was 93.50~104.76%.

**Table 3.** Recovery tests of real samples

Sample	Spiked ( $\mu\text{M}$ )	Total found ( $\mu\text{M}$ )	Recovery (%)
Chili powder	0	0	-
	10	9.35	93.50
	20	20.38	101.90
	30	31.43	104.76

#### 4. CONCLUSIONS

Based on the glassy carbon electrode modified by graphene oxide quantum dots, a simple and effective electrochemical sensor of Rh B was developed. The results show that the sensor has excellent performance in detecting Rh B. under the optimum experimental conditions, the method has a wide detection range (5.0 ~ 50.0  $\mu\text{M}$ ) and a low detection limit (0.80  $\mu\text{M}$ ), and the sensor has the advantages of simple preparation and low cost, and has been successfully applied to the detection of Rh B in chili powder.

#### ACKNOWLEDGEMENT

This work is supported by the Natural Science key funding Program of Xinjiang Uygur Autonomous region University Scientific Research Program (XJEDU2020I016) and the Scientific Research & Innovation Project for postgraduate of Xinjiang Uygur Autonomous region (XJ2022G232).

#### References

1. T. P. Wu, J. C. Zhang, K. Ma, *J. Instrum. Anal.*, 38 (2019) 207.
2. P. H. Duan, Z. H. Li, Y. W. Zhang, K. Ma, *J. Food. Saf. Food. Qual.*, 11 (2020) 6014.
3. X. H. Chen, Y. G. Zhao, H. Y. Shen, M. C. Jin, *J. Chromatogr. A*, 1263 (2012) 34.
4. K. Ma, X. J. Li, H. F. Wang, *Food Anal. Methods.*, 8 (2015) 203.
5. R. W. Mason, I. R. Edwards, *J Chromatogr*, 491 (1989) 468.
6. G. P. Branton, *EFSA J*, 263 (2005) 1.
7. X. L. Zhu, G. L. Wu, C. G. Wang, D. G. Zhang, X. Yuan, *Measurement*, 120 (2018) 206.
8. P. Qi, Z. H. Lin, J. Li, C. L. Wang, W. W. Meng, H. Hong, X. W. Zhang, *Food Chem.*, 164 (2014) 98.
9. Y. E. Unsal, M. Soylak, M. Tuzen, *Desalin Water Treat*, 55 (2015) 2103.
10. J. Wu, W. Liu, R. Zhu, X.S. Zhu, *RSC Adv*, 11 (2021) 8255.
11. R. Khani, S. Sobhani, T. Yari, *Microchem J*, 146 (2019) 471.
12. E. Yilmaz, M. Soylak, *Spectrochim. Acta A Mol. Biomol. Spectrosc.*, 202 (2018) 81.
13. A. A. A. Ahmed Bakheet, X. S. Zhu, *J Fluoresc*, 27 (2017) 1087.
14. R. D. Ji, Z. M. Zhao, X. L. Yu, M. G. Chen, *Optik*, 181 (2019) 796.
15. M. J. Wang, X. L. Nie, L. Tian, J. W. Hu, D. Y. Yin, H. Qiao, T. L. Li, Y. Li, *Food Addit Contam B*, 12 (2019) 59-64.
16. D.W. Chen, Y. F. Zhao, H. Miao, Y. N. Wu, *J Chromatogr A*, 1374 (2014) 268.
17. E. Ates, K. Mittendorf, H. Senyuva, *J Aoac Int*, 94 (2011) 1853.
18. E. Ghasemi, M. Kaykhani, *Spectrochim. Acta A Mol. Biomol. Spectrosc.*, 164 (2016) 93.
19. C. C. Wang, A. N. Masi, L. Fernández, *Talanta*, 75 (2008) 135.
20. G. Kaur, A. Kaur, H. Kaur, *Polym Plast Technol Eng*, 60 (2021) 504.
21. L. J. Xing, W. G. Zhang, L. J. Fu, J. M. Lorenzo, Y. J. Hao, *Food Chem.*, 385 (2022) 132555.
22. N. Kajal, V. Singh, R. Gupta, S. Gautam, *Environ. Res.*, 204 (2022) 112320.
23. V. Karthik, P. Selvakumar, P. S. Kumar, V. Satheeskumar, M. G. Vijaysunder, S. Hariharan, K. Antony, *Chemosphere*, 304 (2022) 135331.
24. L. L. Yu, Y. X. Mao, L. B. Qu, *Food Anal Methods*, 6 (2013) 1665.
25. M. M. Charithra, J. G. Manjunatha, *Mater Chem Phys*, 262 (2021) 124293.
26. X. R. Zhai, S. Li, X. Chen, Y. Hua, H. Wang, *Microchimica Acta*, 187 (2020) 1.
27. J. Zhang, T. Zhang, J. H. Yang, *Ionics*, 28 (2022) 2041
28. J. Zhang, L. Zhang, W. C. Wang, Z. D. Chen, *J Aoac Int*, 99 (2016) 760.

29. D. Sun, X. F. Yang, *Food Anal Methods*, 10 (2017) 2046.
30. Y. H. Yi, H. Sun, G. B. Zhu, X. Y. Wu, *Anal. Methods*, 7 (2015) 4965.
31. M. Saraf, K. Natarajan, A. K. Saini, S. M. Mobin, *Dalton Trans.*, 46 (2017) 15848.
32. L. L. Li, G. H. Wu, G. H. Yang, J. Peng, J. W. Zhao, J. J. Zhu, *Nanoscale*, 5 (2013) 4015.
33. P. He, F. L. Yuan, Z. F. Wang, Z. Tan, L. Fan, *Acta Phys.-Chim. Sin.*, 34 (2018) 1250.
34. P. C. Ooi, J. Lin, T. W. Kim, F. Li, *Org Electron*, 32 (2016) 115.
35. J. Ou, Y. X. Tao, J. J. Xue, Y. Kong, J. Y. Dai, L. H. Deng, *Electrochem Commun*, 57 (2015) 5.
36. A. A. Ensafi, P. Nasr-Esfahani, B. Rezaei, *Sens. Actuators B Chem.* 270 (2018) 192.
37. C. Pothipor, J. Jakmunee, S. Bamrungsap, K. Ounnunkad. *Analyst*, 146 (2021) 4000.
38. X. Li, L. Ni, N. Chen, J. Liu, W. Li, Y. Xian, *Measurement*, 181 (2021) 109566.
39. K. Wu, S. Z. Xu, X. J. Zhou, H. X. Wu, *J. Electrochem.*, 19 (2013) 361.
40. Karimi. B, Ramezanzadeh. B, *J Colloid Interf Sci*, 493 (2017) 62.
41. J. P. Melo, P. L. Ríos, P. Povea, C. Morales-Verdejo, M. B. Camarada, *ACS omega*, 3 (2018) 7278.
42. L. Shi, Z. Wang, L. Bai, G. Yang, *Int. J. Electrochem. Sci*, 17 (2022) 220144.
43. M. L. Wang, J. Zhang, N. N. Ding, X. L. Zhu, Z. D. Chen, *J Aoac Int*, 96 (2013) 625.
44. E. Laviron, *J. Electroanal. Chem. Interfacial Electrochem.*, 52 (1974) 355.
45. S. Ma, Z. D. Chen, *Food Sci Tech-Brazil*, 41 (2016) 284.
46. P. H. Deng, C. Z. Wang, Q. Tang, J. Zeng, Q. Q. Zhu, L. Wen, *J. Hengyang Normal University*, 39 (2018) 60.
47. J. Y. Sun, T. Gan, Y. Li, Z. X. Shi, Y. M. Liu, *J Electroanal Chem*, 724 (2014) 87.